



HAL
open science

The periplasmic coiled coil formed by the assembly platform proteins PulL and PulM is critical for function of the *Klebsiella* type II secretion system

Yuanyuan Li, Javier Santos-Moreno, Olivera Francetic

► To cite this version:

Yuanyuan Li, Javier Santos-Moreno, Olivera Francetic. The periplasmic coiled coil formed by the assembly platform proteins PulL and PulM is critical for function of the *Klebsiella* type II secretion system. *Research in Microbiology*, In press, pp.104075. 10.1016/j.resmic.2023.104075. pasteur-04118037

HAL Id: pasteur-04118037

<https://pasteur.hal.science/pasteur-04118037>

Submitted on 6 Jun 2023

HAL is a multi-disciplinary open access archive for the deposit and dissemination of scientific research documents, whether they are published or not. The documents may come from teaching and research institutions in France or abroad, or from public or private research centers.

L'archive ouverte pluridisciplinaire **HAL**, est destinée au dépôt et à la diffusion de documents scientifiques de niveau recherche, publiés ou non, émanant des établissements d'enseignement et de recherche français ou étrangers, des laboratoires publics ou privés.



Distributed under a Creative Commons Attribution - NonCommercial - NoDerivatives 4.0 International License

Journal Pre-proof



The periplasmic coiled coil formed by the assembly platform proteins PulL and PulM is critical for function of the *Klebsiella* type II secretion system

Yuanyuan Li, Javier Santos-Moreno, Olivera Francetic

PII: S0923-2508(23)00050-5

DOI: <https://doi.org/10.1016/j.resmic.2023.104075>

Reference: RESMIC 104075

To appear in: *Research in Microbiology*

Received Date: 28 September 2022

Revised Date: 25 April 2023

Accepted Date: 26 April 2023

Please cite this article as: Y. Li, J. Santos-Moreno, O. Francetic, The periplasmic coiled coil formed by the assembly platform proteins PulL and PulM is critical for function of the *Klebsiella* type II secretion system, *Research in Microbiology*, <https://doi.org/10.1016/j.resmic.2023.104075>.

This is a PDF file of an article that has undergone enhancements after acceptance, such as the addition of a cover page and metadata, and formatting for readability, but it is not yet the definitive version of record. This version will undergo additional copyediting, typesetting and review before it is published in its final form, but we are providing this version to give early visibility of the article. Please note that, during the production process, errors may be discovered which could affect the content, and all legal disclaimers that apply to the journal pertain.

© 2023 Published by Elsevier Masson SAS on behalf of Institut Pasteur.

1 The periplasmic coiled coil formed by the assembly platform proteins PulL and PulM
2 is critical for function of the *Klebsiella* type II secretion system

3

4 Yuanyuan Li, Javier Santos-Moreno[#], Olivera Francetic^{*}

5

6 Institut Pasteur, Université Paris Cité, CNRS UMR3528, Biochemistry of

7 Macromolecular Interactions Unit, F-75015 Paris, France

8 [#]Present address: University Pompeu Fabra, Department of Medicine and Life
9 Sciences, Barcelona, Spain

10

11

12

13

14

15

16

17

18

19

20

21 Authors' e-mails:

22 Yuanyuan Li: yuanyuan.li@pasteur.fr

23 Javier Santos-Moreno: santosmoreno.j@gmail.com

24 ^{*}Correspondence and reprints: Olivera Francetic: olivera.francetic@pasteur.fr

25

26 **ABSTRACT**

27

28 Bacteria use type II secretion systems (T2SS) to secrete to their surface folded
29 proteins that confer diverse functions, from nutrient acquisition to virulence. In the
30 *Klebsiella* species, T2SS-mediated secretion of pullulanase (PulA) requires assembly
31 of a dynamic filament called the endopilus. The inner membrane assembly platform
32 (AP) subcomplex is essential for endopilus assembly and PulA secretion. AP
33 components PulL and PulM interact with each other through their C-terminal globular
34 domains and transmembrane segments. Here, we investigated the roles of their
35 periplasmic helices, predicted to form a coiled coil, in assembly and function of the
36 PulL–PulM complex. PulL and PulM variants lacking these periplasmic helices were
37 defective for interaction in the bacterial two-hybrid (BACTH) assay. Their functions in
38 PulA secretion and assembly of PulG subunits into endopilus filaments were strongly
39 reduced. Interestingly, deleting the cytoplasmic peptide of PulM nearly abolished the
40 function of variant PulM Δ N and its interaction with PulG, but not with PulL, in the
41 BACTH assay. Nevertheless, PulL was specifically proteolyzed in the presence of the
42 PulM Δ N variant, suggesting that PulM N-terminal peptide stabilizes PulL in the
43 cytoplasm. We discuss the implications of these results for the T2S endopilus and type
44 IV pilus assembly mechanisms.

45

46 **Keywords:**

47 Type II secretion system, Endopilus; type IV pili; assembly platform; pullulanase;
48 *Klebsiella*

49

50

51 **1. Introduction**

52 Bacteria have an astonishing capacity to adapt to diverse environments, growth
53 conditions and nutrient sources. Understanding the molecular basis of this adaptation
54 is fundamentally important and might lead to applications in biotechnology and
55 bioremediation. Among the numerous nanomachines that contribute to bacterial
56 adaptation to diverse environments, type II secretion system (T2SS) plays a prominent
57 role [1].

58 T2SS is typically composed of 15 proteins forming a megadalton complex that
59 spans the envelope of Gram-negative bacteria. Recent reviews summarize our current
60 knowledge of T2SS architecture and function [2, 3]. In the outer membrane, 15
61 subunits of the GspD protein form the secretin channel that allows the passage of large
62 folded proteins or their complexes to the cell surface [4, 5, 6]. According to the current
63 models, protein secretion is driven by the polymerization of periplasmic filaments called
64 endopili (formerly pseudopili, [7]) in the inner membrane. The core of the endopilus is
65 a helical homopolymer composed of the major subunit GspG [8, 9]. The minor pilins
66 GspH, I, J and K form a complex at the endopilus tip [10, 11] and initiate endopilus
67 assembly [12]. The minor pilins are essential for protein secretion and have also been
68 implicated in substrate recognition [13]. Endopili are thought to be continuously
69 polymerized by the inner membrane assembly platform (AP) subcomplex composed
70 of GspF, GspL and GspM proteins [14]. GspL forms a stable complex with the
71 cytoplasmic ATPase GspE [15, 16] and is itself stabilized by GspM [17, 18]. During
72 endopilus elongation, GspM promotes targeting of the GspG and GspH pilins to the
73 AP [19, 20]. In the cytoplasm, cycles of ATP binding and hydrolysis promote
74 conformational changes of the hexameric GspE ATPase complex [21, 22]. These

75 changes are proposed to induce rotational movements of the central AP component
76 GspF that orchestrates endopilus assembly [23].

77 Deciphering the structural basis of endopilus assembly is important to
78 understand how T2SS functions at the molecular level. Structure-function analyses
79 have provided molecular insight into the majority of individual T2SS components.
80 Extending this knowledge towards larger subcomplexes will bring clues on the
81 connectivity and cooperation between the different nanomachine components. So far,
82 cryo-electron microscopy (cryo-EM) has been essential to gain insight into the secretin
83 channel structure [4, 6], a large mostly pentadecameric complex with a periplasmic
84 gate. Combining cryo-EM, nuclear magnetic resonance (NMR), modeling and mass
85 spectrometry provided a detailed view of the pilus core [24, 25] and predicted its
86 connection to the tip complex [26].

87 Recent studies of the *Klebsiella oxytoca* T2SS that secretes pullulanase (PulA)
88 [27] combined X-ray crystallography and NMR to obtain information on the structure of
89 a complex formed between C-terminal domains (CTDs) of PulL (GspL) and PulM
90 (GspM) [28]. Mutations at the interface of these CTDs affect the stability of the two
91 proteins and their function in protein secretion. Cys crosslinking characterized the
92 hydrophobic interface at the membrane level, and led to a model of the PulL – PulM
93 complex (lacking the cytoplasmic domain of PulL) (Fig. 1A). This model predicts
94 additional interactions *via* periplasmic helices of the two partners. Here we investigated
95 the importance of this interface for the formation and function of the PulL – PulM
96 complex. In addition, we studied the role of the short cytoplasmic region of PulM in the
97 stability and function of the AP complex.

98

99 **2. Materials and methods**

100 2.1. Bacterial strains and culture conditions

101 *Escherichia coli* strain DH5 α F'*lacI*^Q was used for cloning and transformation
102 experiments. Functional assays were performed in *E. coli* PAP7460 [29] and PAP5378
103 strains. PAP5378 was constructed by P1 transduction by introducing the *ompT::kan*
104 gene from the Keio collection strain BW2511 *ompT::kan* into strain PAP5299 [12]. The
105 *kan* cassette was then deleted thanks to the helper plasmid pCP20 as described [30]
106 to give strain PAP5299 Δ *ompT*. The bacterial two-hybrid assays were performed in
107 strain DHT1 [31]. Bacteria were grown at 30°C or 37°C in Lysogeny Broth (LB) [32]
108 supplemented with antibiotics as required: ampicillin (Ap) at 100 μ g.mL⁻¹,
109 chloramphenicol (Cm) at 25 μ g.mL⁻¹, Kanamycin (Km) at 25 μ g.mL⁻¹. Solid LB media
110 contained 1.5% agar (Difco). Expression of genes under *lacZ* promoter control was
111 induced with 1 mM isopropyl- β -1-D-thiogalactopyranoside (IPTG). The *pul* gene
112 promoters were induced with 0.4% D-maltose. For secretion assays, media were
113 buffered with 0.1 volume of M63 salt solution [32].

114

115 2.2. Plasmid construction and site-directed mutagenesis

116 Plasmids used in this study are listed in Table 1. Site-directed mutagenesis was
117 performed using a modified QuickChange protocol, with fully overlapping
118 oligonucleotide primers listed in Table S1 (Eurofins). Template DNA was amplified with
119 high fidelity DNA polymerase Q5 (New England Biolabs) in two-steps: first, 6 cycles of
120 amplification were performed with forward and reverse primers alone. The reactions
121 were mixed and another 15 cycles of amplification were performed. The DNA was
122 treated with *DpnI* enzyme (Fermentas) and transformed into DH5 α F' ultracompetent
123 cells prepared as described [33]. Isolated colonies were inoculated into 5 mL of LB
124 with appropriate antibiotics and plasmids were purified using the alkaline lysis protocol

125 and Qiaquick miniprep kit (Qiagen). Plasmids were verified by sequencing (GATC,
126 Eurofins). For the *pull* bacterial two hybrid constructs, vectors pUT18C and pKT25
127 were digested with *EcoRI* and *KpnI* and the purified vector fragments were ligated with
128 the PCR amplified *pull* $\Delta 270-302$ digested the same enzymes. For the *pulM* cloning,
129 the BACTH vectors and PCR fragments were digested with *EcoRI* and *BamHI*.
130 Deletion of *pulM* residues 2-15 in plasmid pCHAP8882 was performed by
131 QuickChange mutagenesis using primers PulM delN5 and PulM delN3 (Table S1). The
132 same approach was used to introduce PulM2-15 deletion in the BACTH constructs
133 pCHAP8154 and pCHAP8155 with primers PulM delN For and PulM delN Rev2 (Table
134 S1).

135

136 2.3. Protein electrophoresis and Western blot analysis

137 Total bacterial extracts were analyzed on denaturing sodium dodecyl-sulphate
138 polyacrylamide gel electrophoresis (SDS-PAGE) using the Tris-tricine gels [34].
139 Proteins were transferred on nitrocellulose membranes using the Fast Blot semi-dry
140 transfer system and one-step transfer buffer (Thermo). Membranes were blocked with
141 5% skim milk in Tris-buffer saline containing 0.05% Tween-20 (TBST) for one hour and
142 probed with primary antibodies diluted in 5% skim milk in TBST. Polyclonal anti-PulM
143 and anti-PulL sera were used at 1:1000 dilution, anti-PulA and anti PulG sera were
144 diluted at 1:2000 and the monoclonal anti-CyaA antibodies were used at 1:10000. After
145 four 10-min washes in TBST, membranes were incubated 1 hour in the secondary goat
146 anti-rabbit or anti-mouse antibodies coupled to horse-radish peroxidase (Amersham)
147 (1:10000). Fluorescence signals were developed with ECL2 (Thermo) and recorded
148 on Typhoon FLA9000 (GE, Cytiva). Chemiluminescence signals were developed with
149 ECL (Thermo) and recorded on an Amersham 680 imager.

150

151

2.4. *PulA* secretion assays

152 Secretion of the non-acylated variant of PulA was assessed by cell fractionation in
153 strain PAP7460 harboring plasmid pCHAP8251 complemented with pCHAP8258
154 derivatives carrying *pull* variants or pCHAP8496 complemented with pCHAP1353
155 derivatives carrying *pulM* variants. Bacteria were cultured overnight at 30°C in LB
156 containing Ap and Cm, then inoculated in inducing medium containing in addition 0.4
157 % D-maltose and 0.1 vol of M63 salts for another 4 hours. Cultures were normalized
158 to OD_{600nm} of 1. Bacterial pellets were collected after 5-min centrifugation at 16000 x g
159 in a table-top Eppendorf centrifuge at 4°C and resuspended in an equal volume of SDS
160 sample buffer. Supernatants were subjected to another 10-min round of centrifugation
161 and 0.1 mL was taken off top, then mixed with 0.1 mL of 2 x SDS sample buffer. Cell
162 and supernatant fractions from the same amount of cultures were analyzed by SDS-
163 PAGE on 10% Tris-glycine gels followed by Western blot with anti-PulA antibodies.
164 PulA bands were quantified with ImageJ and the fraction of PulA in the supernatant
165 was calculated. Data were plotted and analyzed with GraphPad Prism9 software.

166

167

2.5. *PulG* pilus assembly assays

168 To quantify the PulG pilus assembly, bacteria of strain PAP7460 harboring the *pul*
169 operon on plasmid pCHAP8185 and derivatives were cultured for 48 h or 72 h at 30°C
170 on LB plates containing 1.5 % agar (Difco), appropriate antibiotics and 0.2% D-
171 maltose. Bacteria were resuspended in 1 mL of LB and the cell density was normalized
172 to OD_{600nm} of 1. The suspensions were vigorously vortexed for 1 min to detach surface
173 pili. Bacterial pellets were then collected by 5-min centrifugation at 4°C and 16000xg
174 and resuspended in SDS sample buffer at the concentration of 10 OD_{600nm}.mL⁻¹. The

175 pili-containing supernatants were cleared from remaining bacteria by a 10-min
176 centrifugation at 16000xg and 0.7 mL was mixed with tri-chloro-acetic acid at a final
177 concentration of 10%. After a 30-min precipitation on ice, the samples were centrifuged
178 for 30 min at 4°C and 16000 x g. Pellets were washed twice with acetone and air dried,
179 then resuspended in 70 µL of SDS sample buffer. Equivalent volumes were analyzed
180 by SDS-PAGE on 10 % Tris-tricine gels followed by Western blot with anti-PulG
181 antibodies. PulG bands were quantified using ImageJ and the results were analyzed
182 and plotted with Prism 9 software (GraphPad).

183

184 2.6. Bacterial two-hybrid assays

185 Bacterial two-hybrid (BACTH) assay was used to study interactions between
186 proteins fused to T18 and T25 fragments of the CyaA catalytic domain [35]. Plasmids
187 were co-transformed into *E. coli* DHT1 and grown on LB Ap Km plates for 48-60 hours
188 at 30°C. Independent single co-transformants were picked at random, inoculated into
189 1 mL of LB Ap Km and grown overnight at 30°C. These precultures were used to
190 inoculate 1-mL cultures of LB Ap Km containing 1 mM IPTG, which were incubated 4-
191 6 hours at 30°C with shaking. These cultures were used to measure beta-
192 galactosidase activity as described [32]. The data were plotted and analyzed using the
193 Prism 9 software (GraphPad).

194

195 3. Results

196

197 3.1. The periplasmic helices of PulL and PulM are important for T2SS function

198 PulL and PulM share a similar architecture of their transmembrane and periplasmic
199 domains (Fig. 1A). Their hydrophobic alpha-helical transmembrane segments extend
200 into polar periplasmic helices, followed by the flexible linkers connecting them to the
201 ferredoxin-like C-terminal domains (CTDs). The two periplasmic helices are predicted
202 to form a coiled coil [28] (Fig. 1A). To test their functional importance, we generated
203 PulL and PulM variants lacking these periplasmic helices. In PulL, we removed the
204 region comprising residues 270 to 302 (Fig. 1A) to yield variant PulL^{ΔCC}, encoded by
205 plasmid pMS1349 (Table 1). We first tested the ability of PulL^{ΔCC} to promote secretion
206 of the nonacylated variant of pullulanase (PulA), the substrate of the *K. oxytoca* T2SS.
207 Whereas the native PulL (PulL^{WT}) promoted efficient PulA secretion, the majority of the
208 PulA pool accumulated in the cell fraction in the presence of PulL^{ΔCC} (Fig. 1B,C). No
209 extracellular PulA was detected in the negative control lacking PulL. We used
210 antibodies directed against PulL^{CTD} to assess PulL stability in these strains (Fig. 1D).
211 Quantification of PulL^{ΔCC} signals showed that protein levels were reduced by about
212 30% compared to the native PulL (Fig. 1E). The *pulL*^{ΔCC} mutation did not affect PulM
213 levels (Fig. 1F,G).

214 To study the role of the periplasmic helix of PulM, we removed the region
215 comprising residues 37 to 68 (Fig. 1A) resulting in variant PulM^{ΔCC} encoded by plasmid
216 pMS1350 (Table 1). This deletion significantly reduced PulA secretion efficiency (Fig.
217 2A,B), whereas PulM^{ΔCC} stability was reduced by 10% on average compared to PulM
218 (Fig. 2C,D). While PulL levels were reduced in *pulM* mutant, as expected, PulL stability
219 was comparable in *pulM*^{WT} and in the *pulM*^{ΔCC} mutant (Fig. 2E,F).

220

221 *3.2. Pilus assembly defects in pulL^{ACC} and pulM^{ACC} mutants*

222 The AP components PulL and PulM directly participate in endopilus assembly,
223 which is thought to drive PulA secretion. We therefore asked whether the periplasmic
224 helices of PulL and PulM are required for PulG pilus assembly. Under conditions where
225 bacteria are cultured on solid media, *E. coli* harboring a moderate copy-number
226 plasmid encoding a complete set of *pul* genes produces surface pili composed of PulG,
227 the major pilin subunit [36]. We tested the ability of PulL^{ACC} and PulM^{ACC} to restore this
228 function in mutants lacking plasmid-encoded *pulL* (pCHAP8251) or *pulM*
229 (pCHAP8496). After 48 h of growth in the presence of maltose to induce the *pul* gene
230 expression, bacteria complemented with wild type *pulL* and *pulM* genes produced pili
231 that could be sheared from their surface and separated from the cell-associated PulG
232 pool (Fig. 3). In the presence of PulL^{ACC} and PulM^{ACC} variants, the PulG pilus assembly
233 was nearly abolished (Fig. S1). Only upon extending the growth period to 72 h, we
234 could detect some PulG pili on the surface of the coiled coil deletion mutants. Piliation
235 levels were strongly and significantly reduced by the deletions of periplasmic helices
236 (Fig. 3).

237

238 *3.3. The periplasmic coiled coil is required for assembly of the PulL–PulM*
239 *complex*

240 To determine whether the deletion of periplasmic helices affects the PulL–PulM
241 interaction, we used the bacterial two-hybrid (BACTH) assay based on the
242 reconstitution of CyaA adenylyl cyclase signaling pathway [35]. Full-length PulL, PulM
243 and their variants were fused to the C-termini of T18 and T25 CyaA fragments (Table
244 1). The plasmid constructs were co-transformed in *E. coli cya* mutant strain DHT1 to
245 evaluate the reconstitution of adenylyl cyclase activity. By measuring the cAMP-

246 dependent beta-galactosidase activity, we compared interactions of full-length PulL
247 and PulM constructs described previously [28] with constructs harboring the PulL^{ΔCC}
248 and PulM^{ΔCC} variants.

249 Bacteria containing plasmids encoding T18-PulM and T25-PulL showed high
250 beta-galactosidase activity, comparable to that of the yeast leucin zipper positive
251 control, indicating efficient heterodimer formation as observed previously [28] (Fig. 4A).
252 In strains harboring T18-PulM^{ΔCC} and T25-PulL, the mean activity was significantly
253 reduced. Deleting the PulL helix in T25-PulL^{ΔCC} had an even stronger effect and nearly
254 abolished the interaction with T18-PulM. Combining the two deletions in T18-PulM^{ΔCC}
255 and T25-PulL^{ΔCC} slightly increased the mean activity, presumably by placing the
256 respective CTDs at the same level relative to the membrane to facilitate their contacts.
257 However, this increase was weak and not statistically significant in this experimental
258 context (Fig. 4A).

259 Strains harboring the T18-PulL and T25-PulM hybrids showed weaker β-
260 galactosidase activity overall (Fig. 4B), probably due to the generally lower levels of
261 PulL relative to PulM [28]. In this context, beta-galactosidase activity was reduced to
262 background levels upon removal of the periplasmic helix residues in T18-PulL^{ΔCC} or
263 T25-PulM^{ΔCC} and combining the two deletions did not measurably improve the
264 interaction (Fig. 4B). This lack of activity was not due to instability of BACTH constructs,
265 which was verified by Western blot using monoclonal anti-CyaA antibodies directed
266 against T18 fragment (Fig. S2). Overall, the BACTH data suggest that the periplasmic
267 coiled coil - forming regions play a major role in the PulL-PulM assembly.

268

269 *3.4. Periplasmic helix of PulM is not required for binding to PulG*

270 PulM interacts with the pilins PulG and PulH and has been characterized as a
271 targeting factor for these subunits during pilus elongation [19, 20]. Since the deletion
272 of the PulM periplasmic helix affected PulG pilus assembly, we asked whether this was
273 due to an effect on PulM interaction with PulG. The mature portion of PulG fused to
274 the C-terminus of T18 or T25 CyaA fragments was used to probe the interactions with
275 PulM hybrids in the BACTH assay. Although deleting the PulM periplasmic helix
276 reduced the interaction of the T18-PulM – T25-PulG pair, the PulM^{ACC} variant still
277 interacted with PulG strongly and significantly relative to the negative control. In
278 addition, there was no difference in the interaction when T18-PulG was combined with
279 T25-PulM or T25-PulM^{ACC} (Fig. 5A). The β -galactosidase activities of the bacteria co-
280 expressing the *pulG* and *pull* BACTH constructs were at the level of the negative
281 control, indicating no interaction as shown in previous studies [19]. Like the PulL^{WT},
282 the PulL^{ACC} variant did not interact with PulG (Fig. 5B). Based on these data, we
283 concluded that it is unlikely that the piliation defect caused by PulM^{ACC} is due to a
284 defect in PulG binding.

285

286 3.5. *The role of the cytoplasmic PulM peptide*

287 In support of the above conclusion, the PulM-PulG interaction is affected by
288 mutations near the N-terminus of mature PulG [20]. This suggests that the
289 corresponding region of PulM, near the cytoplasmic membrane interface is involved in
290 PulG binding. The cytoplasmic region of PulM is a 16-residue peptide, presumably
291 functioning as a positively charged membrane anchor. We hypothesized that this
292 region interacts with the polar N-terminal residues of PulG, as their substitutions in
293 variants PulG^{T2A} and PulG^{E5A} strongly reduce interactions with PulM [19, 20]. To test
294 this hypothesis, we deleted the cytoplasmic peptide of PulM, and studied interactions

295 of this variant, designated PulM Δ N, with Pull and PulG. In the BACTH assay, the
296 PulM Δ N variant showed a strong and significant defect in binding to PulG, confirming
297 our predictions (Fig. 6A). This defect was comparable to that of PulM binding to the
298 PulG^{E5A} variant, characterized previously [20]. At the same time, deleting the PulM
299 cytoplasmic peptide did not significantly affect its interactions with Pull in this assay.

300 We tested the ability of PulM Δ N to promote Pula secretion and found that nearly
301 all Pula remained cell-bound in the secretion assay, similar to the negative control
302 lacking PulM (Fig. 6B,C). This phenotype is probably caused by the defective
303 interaction of PulM Δ N with PulG. Although the levels of PulM Δ N variant were reduced
304 compared to PulM^{WT}, the protein was still well produced and migrated on SDS-PAGE
305 according to its expected Mw (~16.5 kDa) (Fig. 6D). Interestingly, this variant seemed
306 to form some SDS-resistant dimers that were not detectable with PulM^{WT}. We also
307 tested the levels of Pull in these strains. Surprisingly, although the deletion of PulM
308 N-terminal peptide did not affect its interaction with Pull in the BACTH assay, we found
309 that Pull was strongly destabilized in the presence of PulM Δ N, resulting in a proteolytic
310 product of a size similar to that of PulM (Fig. 6E). Antibodies directed against the
311 Pull^{CTD} detected this product, suggesting that it comprises the inner membrane and
312 periplasmic regions of Pull. As it appears to be generated by a specific cleavage that
313 removes the Pull cytoplasmic domain, we designated this protein Pull Δ N. These
314 results suggest that the PulM cytoplasmic peptide not only ensures PulG targeting to
315 the assembly site through direct interaction, but also protects Pull from specific
316 proteolysis.

317

318 4. Discussion

319

320 Structural information on the PulL_{CTD}–PulM_{CTD} heterodimer, together with the
321 BACTH and cysteine crosslinking data, allowed Dazzoni and collaborators to propose
322 a structural model of membrane-embedded PulL–PulM complex (Fig. 1A) [28].
323 Sequence-based predictions [37] and biochemical data [28] suggest that periplasmic
324 helices of PulL and PulM interact together to form a coiled coil. Our mutational,
325 interaction and functional studies described here support this model and show that this
326 coiled coil plays a major role in PulL–PulM assembly. Deleting residues 270-302 of
327 PulL abolished interaction with PulM in the BACTH assay, and removal of PulM
328 residues 37-68 reduced or abolished PulL binding, depending on the plasmid construct
329 and expression levels. In structural models of PulL and PulM, these deletions would
330 shorten their periplasmic helices by 4.8 nm. This might preclude the interaction of
331 ferredoxin-like CTDs in the deletion variant with the native, full-length partner.
332 Consistent with this model, the BACTH interaction signal was somewhat improved
333 when the two deletions were combined in T18-PulM^{ACC} and T25-PulL^{ACC}. However,
334 this interaction remained weak overall and was not restored to original levels,
335 suggesting that deleted regions play more than just an alignment role. The binding of
336 PulL_{CTD} to PulM_{CTD} is weak and dynamic in solution [28]. Our results show that this
337 interaction is also weak even in the context of PulL^{ACC} or PulM^{ACC} variants, where the
338 two CTDs are anchored in the membrane *via* transmembrane segments followed by
339 their flexible linkers. This suggests that the main role of the coiled coil is to stimulate
340 PulM binding to PulL.

341 When isolated and in solution, PulL_{CTD} and PulM_{CTD} can form different types of
342 parallel and anti-parallel homodimers, as shown by X-ray crystallography [28]. Similar
343 behavior was found for the CTDs of EpsM, the PulM homologue from *V. cholerae* [38]
344 and for XcpL, the PulL homologue from *P. aeruginosa* [39]. Likewise, homo-

345 oligomerization was observed in the ferredoxin-like domains of T4P assembly proteins
346 PilN and PilO, considered as orthologues of Pull transmembrane and periplasmic
347 regions and PulM, respectively. The CTD of PilN from *Thermus thermophilus* [40] and
348 soluble periplasmic regions of *P. aeruginosa* PilO and PilN formed homodimers in
349 crystals [41]. This is in contrast to their poor oligomerization *in vivo* when they are
350 anchored in the bacterial membrane *via* their transmembrane segments, a constraint
351 which reduces the degrees of freedom for CTDs binding.

352 In a yeast two-hybrid study of protein-protein interactions in the *Dickeya dadantii*
353 (formerly *Erwinia chrysanthemi*) T2SS, GspL periplasmic region interacted with the
354 GspM^{CTD} [14] and both periplasmic regions were found to form homo and heterodimers
355 [42]. The recent BACTH data indicate that full-length Pull and PulM preferentially form
356 heterodimers, and that their isolated CTDs interact in a parallel orientation compatible
357 with their membrane insertion [28]. Similarly, full-length *P. aeruginosa* PilN and PilO
358 form heterodimers, with no homodimers observed in the BACTH assay [43]. The long
359 periplasmic helices thus seem to provide a compatible interacting surface to promote
360 efficient formation of the heterodimer coiled coil. Studies in other systems also support
361 the role precise and dynamic interactions between AP components. Mutations in the
362 coiled coil regions of PilN and PilO in the *P. aeruginosa* T4P assembly system cause
363 defects in pilus retraction [44]. In the *Dickeya dadanti* T2SS, the periplasmic regions
364 of OutL and OutM comprise the major interacting interfaces revealed by yeast two-
365 hybrid, BACTH and copurification, although the results of these studies suggested a
366 more prominent role for their CTDs relative to the coiled coil regions [14, 18].

367 In the Pul T2SS, deletions of the Pull and PulM coiled coil regions strongly affected
368 their function. Although variant PulM^{ACC} was more stable and retained the capacity to
369 interact with Pull in the BACTH assay, it was as defective as Pull^{ACC} for both PulA

370 secretion and PulG pilus assembly, suggesting an impaired structure and function of
371 the Pull–PulM complex. The coiled coil might provide structural rigidity to the complex
372 compared to the individual proteins. Shortening of Pull and PulM helices by 4.8 nm
373 could also result in defective interactions with other T2SS components or cellular
374 structures, such as the peptidoglycan layer. In Pull^{ΔCC} and PulM^{ΔCC} variants, the
375 globular ferredoxin-like domains (CTDs) would be placed proximal to the membrane,
376 connected *via* the flexible linkers to the transmembrane helices. This might affect the
377 overall architecture of the T2SS and interactions with its substrates.

378 While we showed here that PulM^{ΔCC} retained its ability to bind PulG, the next step
379 in endopilus assembly, possibly involving binding to Pull, might be impaired. Like in
380 other pilins, the TM segment of PulG is alpha-helical in its membrane-embedded state,
381 but undergoes stretching upon incorporation into the endopilus [25]. This results in the
382 loss of secondary structure in the region between Gly14 and Pro22 of PulG, which
383 adopts an extended coil conformation [25]. The force that causes this stretching is
384 likely to be generated during PulG extraction from the membrane, a key step in
385 endopilus assembly which involves PulG binding to PulM [20]. The Pull–PulM coiled
386 coil might provide an anchoring point during this step. The rigidity or the length of Pull–
387 PulM dimer might be essential to exert force on PulG and operate its stretching during
388 membrane extraction. The PulE ATPase in complex with the Pull cytoplasmic domain
389 might be directly involved in this process. A defect in membrane extraction could be
390 the cause of the major piliation defect observed in *pull*^{ΔCC} and *pulM*^{ΔCC} mutants.

391 Our BACTH data suggest that the PulM cytoplasmic region is not essential for
392 interaction with Pull, and that the periplasmic regions play a dominant role. The
393 specific cleavage of Pull cytoplasmic domain in the *pulMΔN* mutant was therefore
394 surprising. We hypothesize that the N-terminal peptide of PulM protects Pull from

395 proteolysis by binding to a disordered linker that connects PulL_{cyto} domain with the
396 transmembrane and periplasmic regions. This linker is present in the PulL model
397 retrieved from the AF2 database [45] and predicted by the Alpha Fold 2 algorithm [46]
398 (Fig. S3).

399 Binding to the disordered PulL linker might require the free N-terminus of PulM, and
400 thus might occur in the native context, but not in the BACTH constructs, where PulM
401 N-terminus is fused to the T18 and T25 CyaA fragments. A similar interaction is
402 observed in T4P assembly systems, between the conserved N-terminal peptide of PilN
403 and PilM, which is an orthologue of the PulL_{cyto} domain [47, 48]. This contact is highly
404 important for pilus assembly [49] and involves a conserved sequence Φ NLLP (where
405 Φ is a V, I or L) at the N-terminus of PilN homologues. Structural studies have shown
406 that this N-terminal peptide fits into a groove in PilM, allowing them to form a stable
407 PilM–PilN complex – a functional equivalent of PulL. The conserved Asn residue (N5
408 in PilN of *T. thermophilus*) plays a major role in PilM binding by forming a network of
409 hydrogen bonds with several residues in the PilM groove [47]. Functional data support
410 the crucial role of its equivalent Asn8 in the *Neisseria meningitidis* PilN, reflected by
411 the strong piliation defect of the PilN^{N8A} variant [49]. Although not conserved in the
412 GspM homologues, the presence of a similar N-terminal sequence in PulM, **MH**NLL****
413 (identical residues shown in bold) led us to test the effect of N3A substitution in PulM.
414 The PulM^{N3A} variant showed a strong secretion defect and affected the stability of both
415 PulM and PulL [28]. Similar effects were observed in the PulM Δ N variant described
416 here. The *pulM Δ N* mutants show reduced PulM and PulL stability, generating a distinct
417 PulL fragment corresponding in size and likely in domain organization to the PilN
418 component of T4P assembly systems. Of note, a similar PulL degradation product is
419 also observed in the presence of native PulM [28], suggesting that the cytoplasmic

420 linker region of PulL is dynamic and protease sensitive, even in the presence of its
421 interacting partner(s).

422 The above results argue that, although PulM is often considered as an orthologue
423 of PilO in T4P systems, its role may be more similar to that of PilN. Importantly, direct
424 interaction of PulM with the major pilin PulG parallels the binding of the PilN homologue
425 HofN to the major pilin PpdD in the T4P assembly system of Enterohaemorrhagic *E.*
426 *coli* [50].

427 The N-terminal regions of PulM and PilN might therefore play analogous roles in
428 pilin targeting to the assembly site. The phenotype of the PulM Δ N variant, strongly
429 defective in PulG binding and affecting PulL stability, suggests a role of the cytoplasmic
430 PulM peptide in passing the pilin subunits to PulL for incorporation into the growing
431 pilus. PulM is also more abundant in the cell relative to PulL [28] consistent with its role
432 as a shuttle between the large membrane pool of free PulG and the PulL protein stably
433 bound to the ATPase PulE at the endopilus assembly site. Crosslinking studies of *V.*
434 *cholerae* T2SS provided evidence for a transient complex of EpsL with EpsG [51],
435 supporting at least a transient formation of G-M-L tripartite complex. Clearly, further
436 studies are needed to identify their precise interactions within this complex and
437 conformational changes of partners that promote this key step during endopilus
438 assembly.

439

440

441 **Conflict of interest statement**

442 The authors declare that they have no conflict of interest.

443

444 **Acknowledgments**

445 This work was funded by Institut Pasteur, CNRS and ANR grant Synergy-T2SS ANR-
446 19-CE11-0020-01. We are grateful to R. Ieva, R. Voulhoux, N. Izadi-Pruneyre and E.
447 Bouveret for critical reading of the manuscript. We thank I. Guilvout and members of
448 the BIM unit for helpful discussions. YL was a student of the Pasteur Paris University
449 (PPU) international PhD program. JSM was funded by a fellowship from the Basque
450 Government.

451

452 **References**

453

- 454 [1] Cianciotto NP, White RC. Expanding Role of Type II Secretion in Bacterial Pathogenesis
455 and Beyond. *Infect Immun*. 2017;85:e00014-17.
- 456 [2] Gu S, Shevchik VE, Shaw R, Pickersgill RW, Garnett JA. The role of intrinsic disorder and
457 dynamics in the assembly and function of the type II secretion system. *Biochim Biophys Acta*
458 (BBA) - Proteins and Proteomics. 2017;1865:1255-66.
- 459 [3] Naskar S, Hohl M, Tassinari M, Low HH. The structure and mechanism of the bacterial type
460 II secretion system. *Mol Microbiol*. 2021;115:412-24.
- 461 [4] Yan Z, Yin M, Xu D, Zhu Y, Li X. Structural insights into the secretin translocation channel
462 in the type II secretion system. *Nat Struct Mol Biol* 2017;24: 177–83.
- 463 [5] Hay I. D, J. BM, Lithgow T. Structural Basis of Type 2 Secretion System Engagement
464 between the Inner and Outer Bacterial Membranes. *mBio*. 2017;8:e01344-17.
- 465 [6] Chernyatina AA, Low HH. Core architecture of a bacterial type II secretion system. *Nat*
466 *Commun*. 2019;10:5437.
- 467 [7] Wang F, Craig L, Liu X, Rensing C, Egelman EH. Microbial nanowires: type IV pili or
468 cytochrome filaments? *Trends in microbiology*. 2022.
- 469 [8] Sauvonnnet N, Gounon P, Pugsley AP. PpdD type IV pilin of *Escherichia coli* K-12 can be
470 assembled into pili in *Pseudomonas aeruginosa*. *J Bacteriol*. 2000;182:848-54.
- 471 [9] Kohler R, Schafer K, Muller S, Vignon G, Diederichs K, Philippsen A, et al. Structure and
472 assembly of the pseudopilin PulG. *Mol Microbiol*. 2004;54:647-64.
- 473 [10] Korotkov KV, Hol WGJ. Structure of the GspK–GspI–GspJ complex from the
474 enterotoxigenic *Escherichia coli* type 2 secretion system. *Nature structural & molecular*
475 *biology*. 2008;15:462-8.
- 476 [11] Douzi B, Durand E, Bernard C, Alphonse S, Cambillau C, Filloux A, et al. The XcpV/GspI
477 pseudopilin has a central role in the assembly of a quaternary complex within the T2SS
478 pseudopilus. *J Biol Chem*. 2009;284:34580-9.
- 479 [12] Cisneros DA, Bond PJ, Pugsley AP, Campos M, Francetic O. Minor pseudopilin self-
480 assembly primes type II secretion pseudopilus elongation. *The EMBO J*. 2012;31:1041-53.
- 481 [13] Douzi B, Ball G, Cambillau C, Tegoni M, Voulhoux R. Deciphering the Xcp *Pseudomonas*
482 *aeruginosa* Type II Secretion Machinery through Multiple Interactions with Substrates. *J Biol*
483 *Chem*. 2011;286:40792-801.
- 484 [14] Py B, Loiseau F, Barras F. An inner membrane platform in the type II secretion machinery
485 of Gram-negative bacteria. *EMBO Rep*. 2001;2:244–8.
- 486 [15] Py B, Loiseau L, Barras F. Assembly of the type II secretion machinery of *Erwinia*
487 *chrysanthemi*: direct interaction and associated conformational change between OutE, the

- 488 putative ATP-binding component and the membrane protein OutL. *J Mol Biol.* 1999;289:659-
489 70.
- 490 [16] Abendroth J, Murphy P, Sandkvist M, Bagdasarian M, Hol WG. The X-ray structure of the
491 type II secretion system complex formed by the N-terminal domain of EpsE and the
492 cytoplasmic domain of EpsL of *Vibrio cholerae*. *J Mol Biol.* 2005;348:845-55.
- 493 [17] Sandkvist M, Hough LP, Bagdasarian MM, Bagdasarian M. Direct interaction of the EpsL
494 and EpsM proteins of the general secretion apparatus in *Vibrio cholerae*. *J Bacteriol.*
495 1999;181:3129-35.
- 496 [18] Lallemand M, Login FH, Guschinskaya N, Pineau C, Effantin G, Robert X, et al. Dynamic
497 Interplay between the Periplasmic and Transmembrane Domains of GspL and GspM in the
498 Type II Secretion System. *PLoS One.* 2013;8:e79562.
- 499 [19] Nivaskumar M, Santos-Moreno J, Malosse C, Nadeau N, Chamot-Rooke J, Tran Van
500 Nhieu G, et al. Pseudopilin residue E5 is essential for recruitment by the type 2 secretion
501 system assembly platform. *Mol Microbiol.* 2016;101:924-41.
- 502 [20] Santos-Moreno J, East A, Guilvout I, Nadeau N, Bond PJ, Tran Van Nhieu G, et al. Polar
503 N-terminal Residues Conserved in Type 2 Secretion Pseudopilins Determine Subunit
504 Targeting and Membrane Extraction Steps during Fibre Assembly. *J Mol Biol.* 2017;429:1746-
505 65.
- 506 [21] Robien MA, Krumm BE, Sandkvist M, Hol WG. Crystal structure of the extracellular protein
507 secretion NTPase EpsE of *Vibrio cholerae*. *J Mol Biol.* 2003;333:657-74.
- 508 [22] Patrick M, Korotkov KV, Hol WGJ, Sandkvist M. Oligomerization of EpsE Coordinates
509 Residues from Multiple Subunits to Facilitate ATPase Activity. *J Biol Chem.* 2011;286:10378-
510 86.
- 511 [23] Nivaskumar M, Bouvier G, Campos M, Nadeau N, Yu X, Egelman EH, et al. Distinct
512 Docking and Stabilization Steps of the Pseudopilin Conformational Transition Path Suggest
513 Rotational Assembly of Type IV Pilus-like Fibers. *Structure.* 2014;22:685-96.
- 514 [24] Campos M, Nilges M, Cisneros M, Francetic O. Detailed structure and assembly model of
515 the type II secretion pilus from sparse data. *Proc Natl Acad Sci USA.* 2010;107:13081-6.
- 516 [25] López-Castilla A, Thomassin J-L, Bardiaux B, Zheng W, Nivaskumar M, Yu X, et al.
517 Structure of the calcium-dependent type 2 secretion pseudopilus. *Nat Microbiol.* 2017;2:1686-
518 95.
- 519 [26] Escobar CA, Douzi B, Ball G, Barbat B, Alphonse S, Quinton L, et al. Structural interactions
520 define assembly adapter function of a type II secretion system pseudopilin. *Structure.*
521 2021;29:1116-27.e8.
- 522 [27] Michaelis S, Chapon C, d'Enfert C, Pugsley AP, Schwartz M. Characterization and
523 expression of the structural gene for pullulanase, a maltose-inducible secreted protein of
524 *Klebsiella pneumoniae*. *J Bacteriol.* 1985;164:633-8.
- 525 [28] Dazzoni R, Li Y, López-Castilla A, Brier S, Mechaly A, Cordier F, et al. Structure and
526 dynamic association of an assembly platform subcomplex of the bacterial type II secretion
527 system. *Structure.* 2023;31:152-65.e7.
- 528 [29] Possot O, Vignon G, Bomchil N, Ebel F, Pugsley AP. Multiple interactions between
529 pullulanase secretion components involved in stabilization and cytoplasmic membrane
530 association of PulE. *J Bacteriol.* 2000;182:2142-52.
- 531 [30] Datsenko KA, Wanner BL. One-step inactivation of chromosomal genes in *Escherichia*
532 *coli* K-12 using PCR products. *Proc Natl Acad Sci U S A.* 2000;97:6640-5.
- 533 [31] Dautin N, Karimova G, Ullmann A, Ladant D. Sensitive Genetic Screen for Protease
534 Activity Based on a Cyclic AMP Signaling Cascade in *Escherichia coli*. *J Bacteriol.*
535 2000;182:7060-6.
- 536 [32] Miller JH. *Experiments in Molecular Genetics.*: Cold Spring Harbor Laboratory, Cold
537 Spring Harbor, NY. USA; 1972.
- 538 [33] Inoue H, Nojima H, Okayama H. High efficiency transformation of *Escherichia coli* with
539 plasmids. *Gene.* 1990;96:23-8.
- 540 [34] Schägger H, von Jagow G. Tricine-sodium dodecyl sulfate-polyacrylamide gel
541 electrophoresis for the separation of proteins in the range from 1 to 100 kDa. *Anal Biochem.*
542 1987;166:368-79.

- 543 [35] Karimova G, Pidoux J, Ullmann A, Ladant D. A bacterial two-hybrid system based on a
544 reconstituted signal transduction pathway. *Proc Natl Acad Sci U S A*. 1998;95:5752-6.
- 545 [36] Sauvonnet N, Vignon G, Pugsley AP, Gounon P. Pilus formation and protein secretion by
546 the same machinery in *Escherichia coli*. *EMBO J*. 2000;19:2221-8.
- 547 [37] Ludwiczak J, Winski A, Szczepaniak K, Alva V, Dunin-Horkawicz S. DeepCoil—a fast and
548 accurate prediction of coiled-coil domains in protein sequences. *Bioinformatics (Oxford, England)*. 2019;35:2790-5.
- 549 [38] Abendroth J, Rice AE, McLuskey K, Bagdasarian M, Hol WG. The crystal structure of the
550 periplasmic domain of the type II secretion system protein EpsM from *Vibrio cholerae*: the
551 simplest version of the ferredoxin fold. *J Mol Biol*. 2004;338:585-96.
- 552 [39] Fulara A, Vandenberghe I, Read RJ, Devreese B, Savvides SN. Structure and
553 oligomerization of the periplasmic domain of GspL from the type II secretion system of
554 *Pseudomonas aeruginosa*. *Sci Rep*. 2018;8:16760.
- 555 [40] Karuppiyah V, Collins RF, Thistlethwaite A, Gao Y, Derrick JP. Structure and assembly of
556 an inner membrane platform for initiation of type IV pilus biogenesis. *Proc Natl Acad Sci USA*.
557 2013;110:E4638-E47.
- 558 [41] Sampaleanu LM, Bonanno JB, Ayers M, Koo J, Tammam S, Burley SK, et al. Periplasmic
559 Domains of *Pseudomonas aeruginosa* PilN and PilO Form a Stable Heterodimeric Complex.
560 *J Mol Biol*. 2009;394:143-59.
- 561 [42] Douet V, Loiseau L, Barras F, Py B. Systematic analysis, by the yeast two-hybrid, of
562 protein interaction between components of the type II secretory machinery of *Erwinia*
563 *chrysanthemi*. *Research in microbiology*. 2004;155:71-5.
- 564 [43] Leighton TL, Dayalani N, L.M. S, Howell PL, LL. B. Novel Role for PilNO in Type IV Pilus
565 Retraction Revealed by Alignment Subcomplex Mutations. *J Bacteriol*. 2015;197:2229-38.
- 566 [44] Leighton TL, Yong DH, Howell PL, Burrows LL. Type IV Pilus Alignment Subcomplex
567 Proteins PilN and PilO Form Homo- and Heterodimers *n Vivo*. *J Biol Chem*. 2016;291:19923-
568 38.
- 569 [45] Varadi M, Anyango S, Deshpande M, Nair S, Natassia C, Yordanova G, et al. AlphaFold
570 Protein Structure Database: massively expanding the structural coverage of protein-sequence
571 space with high-accuracy models. *Nucl Acids Res*. 2022;50:D439-D44.
- 572 [46] Jumper J, Evans R, Pritzel A, Green T, Figurnov M, Ronneberger O, et al. Highly accurate
573 protein structure prediction with AlphaFold. *Nature*. 2021;596:583-9.
- 574 [47] Karuppiyah V, Derrick JP. Structure of the PilM-PilN Inner Membrane Type IV Pilus
575 Biogenesis Complex from *Thermus thermophilus*. *J Biol Chem*. 2011;286:24434-42.
- 576 [48] McCallum M, Tammam S, Little DJ, Robinson H, Koo J, Shah M, et al. PilN Binding
577 Modulates the Structure and Binding Partners of the *Pseudomonas aeruginosa* Type IVa Pilus
578 Protein PilM*. *J Biol Chem*. 2016;291:11003-15.
- 579 [49] Georgiadou M, Castagnini M, Karimova G, Ladant D, Pelicic V. Large-scale study of the
580 interactions between proteins involved in type IV pilus biology in *Neisseria meningitidis*:
581 characterization of a subcomplex involved in pilus assembly. *Mol Microbiol*. 2012;84:857-73.
- 582 [50] Luna Rico A, Zheng W, Petiot N, Egelman EH, Francetic O. Functional reconstitution of
583 the type IVa pilus assembly system from enterohaemorrhagic *Escherichia coli*. *Mol Microbiol*.
584 2019;111:732-49.
- 585 [51] Gray MD, Bagdasarian M, Hol WGJ, Sandkvist M. In vivo cross-linking of EpsG to EpsL
586 suggests a role for EpsL as an ATPase-pseudopilin coupling protein in the Type II secretion
587 system of *Vibrio cholerae*. *Mol Microbiol*. 2011;79:786-98.
- 588
- 589
- 590

592 **Table 1. Plasmids used in this study**

| Name | Relevant characteristics | Source/Reference |
|-----------|--|------------------|
| pCHAP8185 | <i>pulC-O, pulAB, pulS, Ap^R, ColE1 ori</i> | [12] |
| pCHAP8496 | pCHAP8185 $\Delta pulM$ | [20] |
| pCHAP8251 | pCHAP8185 $\Delta pull$ | [20] |
| pCHAP8258 | <i>placZ-pull, Cm^R, p15A ori</i> | [20] |
| pMS1349 | pCHAP8258 <i>pull</i> Δ 270-302 (<i>pull</i> ^{ΔCC}), | This study |
| pCHAP1353 | <i>placZ-pulM, Cm^R, p15A ori</i> | [29] |
| pMS1350 | pCHAP8258 <i>pulM</i> Δ 37-68 (<i>pulM</i> ^{ΔCC}), | This study |
| | <i>pulM</i> Δ 2-15 (<i>pulM</i> Δ N) Cm ^R , p15A ori | This study |
| pCHAP8882 | <i>cyaT18 Ap^R, ColE1 ori</i> | This study |
| pUT18C | <i>cyaT25 Km^R, p15A ori</i> | [35] |
| pKT25 | | [35] |
| pMS1222 | <i>T18-pull Ap^R, ColE1 ori</i> | [28] |
| pMS1229 | <i>T25-pull, Km^R, p15A ori</i> | [28] |
| pCHAP8154 | <i>T18-pulM, Ap^R, ColE1 ori</i> | [19] |
| pCHAP8155 | <i>T25-pulM, Km^R, p15A ori</i> | [19] |
| pMS1355 | <i>T18-pull</i> Δ 270-302, Ap ^R , ColE1 ori | This study |
| pMS1356 | <i>T25-pull</i> Δ 270-302, Km ^R , p15A ori | This study |
| pMS1357 | <i>T18-pulM</i> Δ 37-68 Ap ^R , ColE1 ori | This study |
| pMS1358 | <i>T25-pulM</i> Δ 37-68 Km ^R , p15A ori | This study |
| pCHAP7330 | <i>T18-pulG, Ap^R, ColE1 ori</i> | [23] |
| pCHAP7332 | <i>T25-pulG, Km^R, p15A ori</i> | [23] |
| pMS1147 | <i>T18-pulM</i> Δ 2-15 Ap ^R , ColE1 ori | This study |
| pMS1148 | <i>T25-pulM</i> Δ 2-15 Km ^R , p15A ori | This study |

594

595 **Figure legends**

596

597 **Figure 1.** Deletion of the PulL periplasmic helix affects PulA secretion. **A.** Schematic
598 view of the PulL-PulM dimer in the inner membrane (IM). PulL is shown in green with
599 its periplasmic helix in lime; PulM is shown in magenta and its periplasmic helix in pale
600 pink. The numbers indicate positions of residues (shown as spheres) at the boundaries
601 of deleted segments in PulL ^{Δ CC} (270-302) and PulM ^{Δ CC} (37-68). **B.** Secretion of PulA
602 in strains producing native PulL (WT), no PulL (Δ L) and PulL ^{Δ CC}. PulA secretion assay
603 was performed (Materials and Methods) and 0.005 OD_{600nm} equivalents of cell- (CF)
604 and supernatant fractions (SN) were analyzed by Western blot with anti-PulA
605 antibodies. **C.** PulA secretion efficiency quantified from 3 independent assays as in
606 **(B)**. The column height shows the mean values and dots represent values from

607 independent experiments. **D.** Concentrated cell fractions (from 0.05 OD_{600nm} of
608 bacteria) as in (**B**) analyzed with anti-PulL antibodies. **E.** Mean relative levels of PulL
609 quantified from concentrated cell fractions of strains from 3 independent experiments
610 (black dots) as in (**D**). Bar graphs indicate mean signal intensities of bands detected
611 with anti-PulL antibodies in strains producing PulL^{WT} and PulL^{ACC}. Mean levels of
612 PulL^{ACC} signal relative to PulL^{WT} are indicated above the bar. **F.** Concentrated cell
613 fractions from 0.05 OD_{600nm} of bacteria as in (**D**), analyzed with anti-PulM antibodies.
614 **G.** Relative levels of PulM quantified from 3 independent experiments as in (**F**). Bar
615 heights indicate mean signal intensities and dots indicate individual values. Statistical
616 analysis was performed with Prism9 (GraphPad) using ordinary one-way ANOVA with
617 multiple comparisons. ****, p<0.0001, ns (non-significant difference). Nonspecific
618 bands cross-reacting with anti-PulL and anti-PulM antibodies are indicated by a star.

619

620 **Figure 2.** PulM periplasmic helix region is required for full T2SS function. **A.** Secretion
621 of PulA in strains producing native PulM (WT), no PulM (Δ M) and PulM^{ACC}. PulA
622 secretion assay was performed and 0.005 OD_{600nm} equivalents of cell- (CF) and
623 supernatant fractions (SN) were analyzed by Western blot with anti-PulA antibodies.
624 **B.** PulA secretion efficiency quantified from 3 independent assays in the presence of
625 PulM (WT) or PulM^{ACC} and without PulM (Δ M). Bar heights show the mean values and
626 dots represent values from 4 independent experiments. **C.** Cell fractions from 0.05
627 OD_{600nm} of bacteria as in (**A**) probed with anti-PulM antibodies. **D.** Signal intensities of
628 bands detected with anti-PulM antibodies from 3 independent sample as in (**C**) (black
629 dots). Bar heights indicate mean signal intensity and error bars show standard
630 deviations. Mean levels of PulM^{ACC} signal relative to PulM^{WT} are indicated above the
631 bar. **E.** Concentrated cell fractions of samples as in (**C**) from 0.05 OD_{600nm} of bacteria,

632 analyzed with anti-PuL antibodies. **F.** Relative levels of PuL quantified from 3
633 independent experiments as in **(E)**. Bar heights indicate mean signal intensities, dots
634 indicate individual values and error bars show standard deviation. Statistical analysis
635 was performed using ordinary one-way ANOVA with multiple comparisons. *, $p < 0.05$;
636 **, $p < 0.01$, ns (non-significant difference).

637

638

639 **Figure 3.** Piliation defect of PuL and PuM lacking periplasmic helices. PuLG pilus
640 assembly on the surface of PAP7460 bacteria containing plasmid pCHAP8251
641 complemented with pCHAP8252 (PuL^{WT}), pMS1348 (PuL^{ΔCC}) or vector pSU19 (ΔL),
642 or PAP7460 containing plasmid pCHAP8496 complemented with pCHAP1353
643 (PuM^{WT}), pMS1350 (PuM^{ΔCC}) or vector pSU18 (ΔM). Percentage of PuLG present in
644 the sheared fractions (SF) from bacteria cultured for 72 h at 30°C as described in
645 Materials and Methods. Bar heights represent mean values from five independent
646 piliation experiments (dots) and error bars indicate standard deviation. Statistical
647 analysis was performed by one-way ANOVA with multiple comparisons. ****,
648 $p < 0.0001$, ns (non-significant difference).

649

650 **Figure 4.** Periplasmic helices are required for PuL – PuM interaction. **A.** Analysis of
651 interactions between T18-PuM with T25-PuL and their derivatives. **B.** Analysis of
652 interactions between T18-PuL with T25-PuM and their derivatives. Beta-
653 galactosidase activity (Miller units) of DHT1 bacteria co-transformed with plasmids
654 producing T18 and T25 or their hybrids as indicated: Z, yeast leucine zipper; M (PuM),
655 L (PuL); M^{ΔCC} (PuM^{ΔCC}) and L^{ΔCC} (PuL^{ΔCC}). The bar graph heights indicate mean
656 values and error bars show standard deviation. Black dots show β-gal. activities of
657 individual cultures. Statistical analysis was performed with GraphPad Prism 9 using

658 One-way ANOVA test with multiple comparisons. ****, $p < 0.0001$; ns (no significant
659 difference).

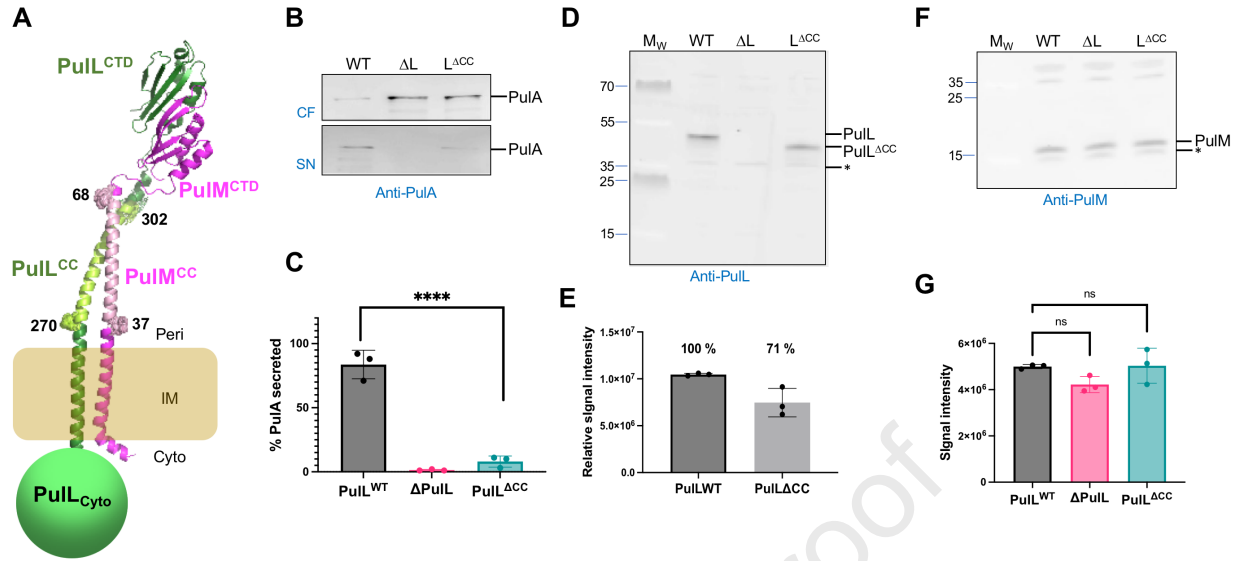
660

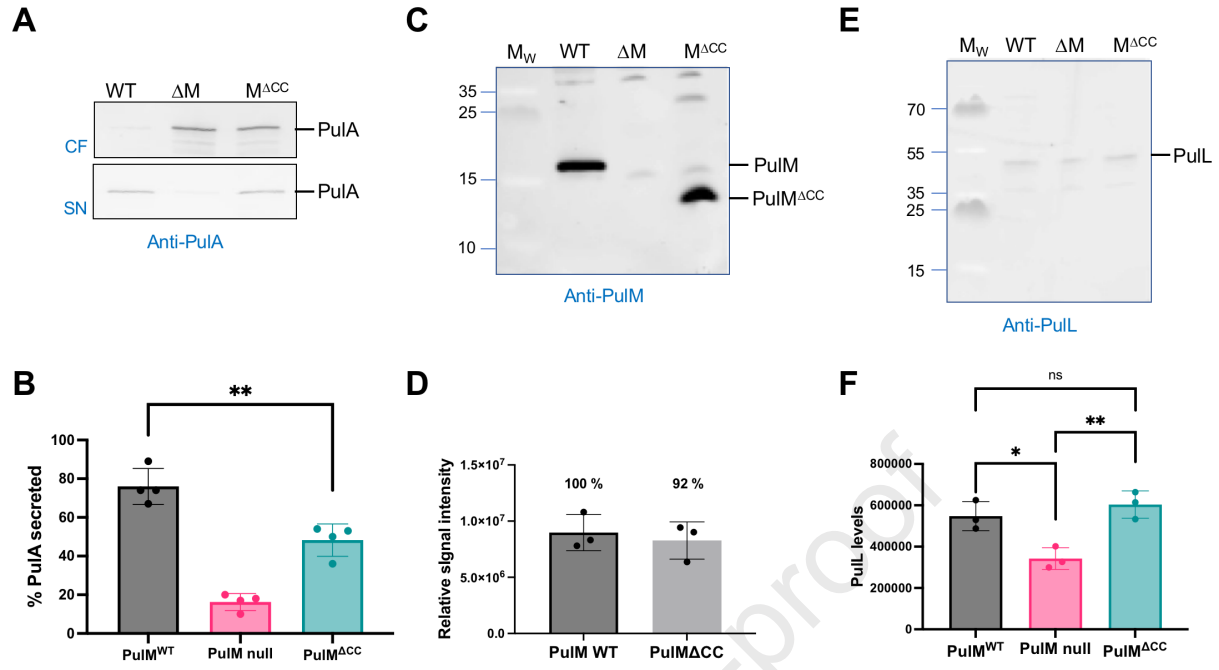
661 **Figure 5.** PulM periplasmic α -helix is not essential for interaction with PulG. **A.**
662 Interaction analysis of PulG with PulM and derivatives. **B.** Interaction analysis of PulG
663 with PulL and derivatives. Beta galactosidase activity measured for indicated pairs of
664 T18- and T25- hybrids. Z, yeast leucine zipper; M (PulM), L (PulL); M Δ CC (PulM Δ CC),
665 L Δ CC (PulL Δ CC) and G (PulG). Bar graphs indicate mean values and error bars
666 standard deviation. Black dots show activity values of independent cultures ($n \geq 4$). The
667 data were plotted and analyzed with GraphPad Prism 9 software, using one-way
668 ANOVA test with multiple comparisons. ****, $p < 0.0001$, ns (non-significant difference).

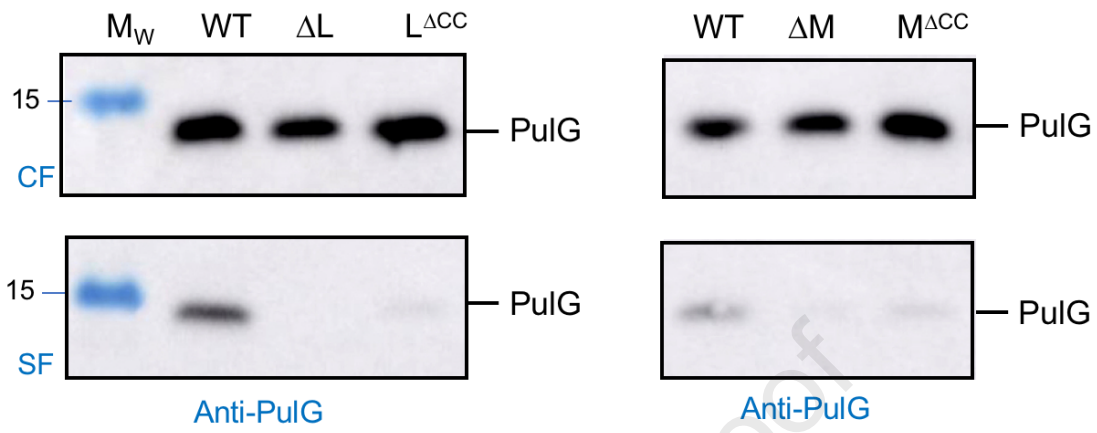
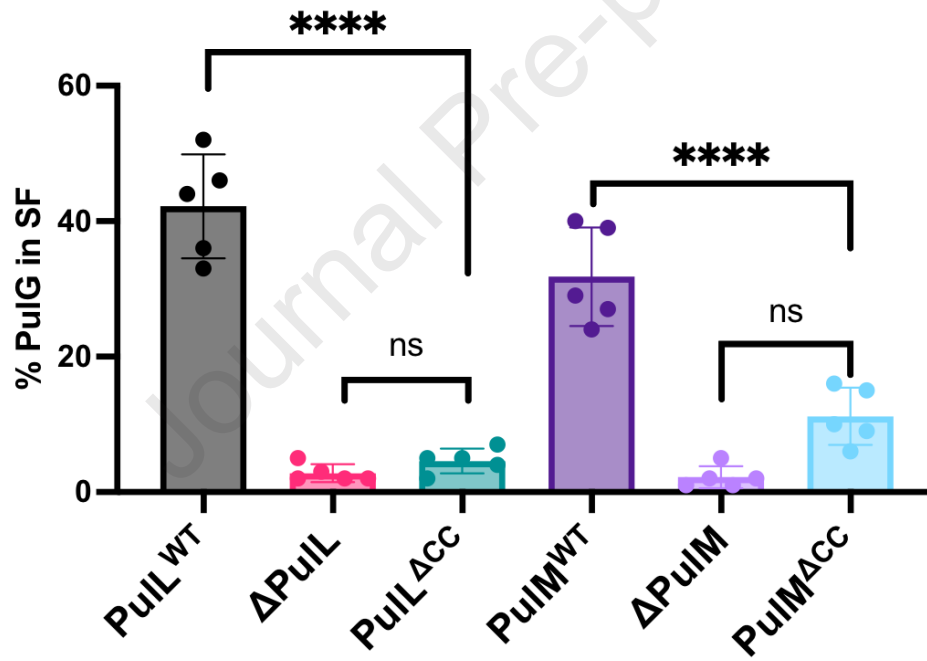
669

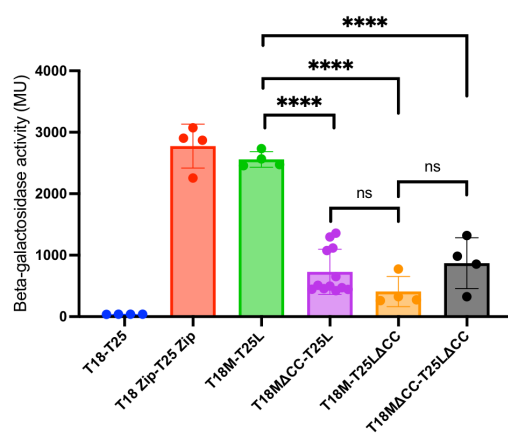
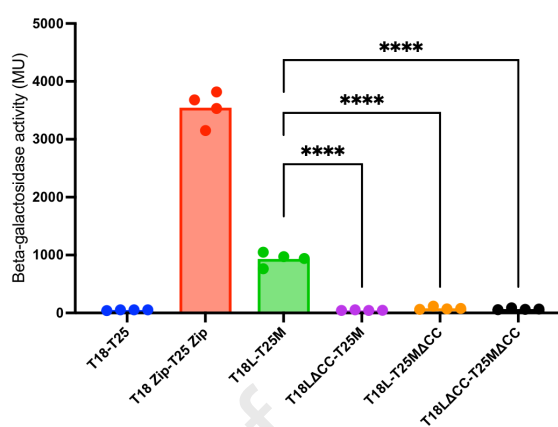
670 **Figure 6.** PulM cytoplasmic peptide is essential for interaction with PulG and for the
671 PulL stability. **A.** BACTH analysis of PulM and PulM Δ N interactions with PulG and PulL
672 Black dots show beta-galactosidase activity values of 4 independent cultures and bar
673 graphs indicate mean activities. Statistical analysis was performed by one-way
674 ANOVA with multiple comparisons. ****, $p < 0.0001$, ns (non-significant difference). **B.**
675 PulA secretion assay in strain PAP5378 containing plasmid pCHAP8496 (Δ pulM)
676 complemented with *pulM*^{WT} (on pCHAP1353), *pulM* Δ N (on pCHAP8882) and empty
677 vector pSU18 (Δ pulM). Secretion assay was performed as described in Materials and
678 Methods. **C.** Quantification of secreted PulA fraction (%) from three independent
679 assays as in (B). (D) PulM and (E) PulL levels in strain PAP7460 carrying pCHAP8496
680 (Δ pulM) complemented with *pulM*^{WT} (on pCHAP1353), empty vector (pSU18) and
681 *pulM* Δ N (on pCHAP8882). The asterisk in (D) marks a nonspecific band cross-reacting
682 with the anti-PulM antibody.

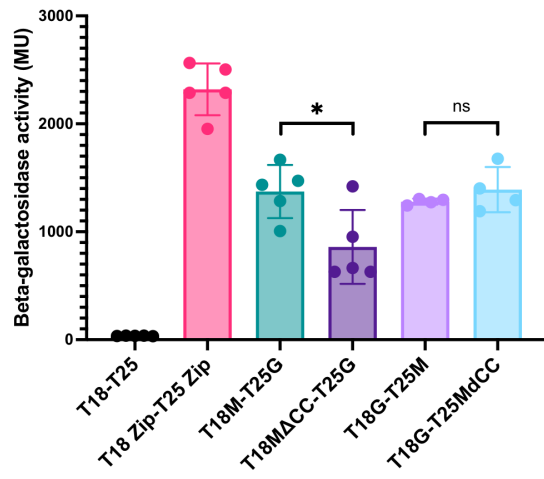
Journal Pre-proof





A**B**

A**B**

A**B**